Cancer Chemotherapy and Pharmacology (2020) 85:293–308
https://doi.org/10.1007/s00280-019-04001-2

ORIGINAL ARTICLE

Population pharmacokinetic analysis of intravenous busulfan: *GSTA1* genotype is not a predictive factor of initial dose in Chinese adult patients undergoing hematopoietic stem cell transplantation

Yidan Sun[1] · Jingjing Huang[2] · Chenxia Hao[2] · Ziwei Li[3] · Wu Liang[4] · Weixia Zhang[2] · Bing Chen[2] · Wanhua Yang[2] · Jiong Hu[1]

Received: 9 August 2019 / Accepted: 22 November 2019 / Published online: 13 December 2019

Abstract

Purpose This study aimed to develop a population pharmacokinetic (PPK) model to investigate the impact of *GSTA1, GSTP1,* and *GSTM1* genotypes on busulfan pharmacokinetic (PK) variability in Chinese adult patients.

Methods Forty-three and 19 adult patients who underwent hematopoietic stem cell transplantation (HSCT) were enrolled for modeling group and validation group, respectively. All patients received twice-daily intravenous busulfan as part of conditioning regimen before HSCT. The PPK model was developed by nonlinear mixed-effect modeling. Covariates investigated were age, sex, actual body weight, body surface area, diagnoses, hepatic function markers, *GST* genotypes and conditioning regimen.

Results A total of 488 busulfan concentrations from 43 patients were obtained for the PPK model. The PK of intravenous busulfan was described by one-compartment model with first-order elimination with estimated clearance (CL) of 14.2 L/h and volume of distribution of 64.1 L. Inclusion of *GSTA1* genotype as a covariate accounted for 1.1% of the inter-individual variability of busulfan CL (from 17.8% in the basic model to 16.7% in the final model). The accuracy and applicability of the final model were externally validated in the independent group. The difference of busulfan PK between Chinese patients and Caucasian patients existed because of the rarity of haplotype **B* in Chinese population.

Conclusions Although the *GSTA1* genotype-based PPK model of intravenous busulfan was successfully developed and externally validated, the *GSTA1* genotype was not considered to be clinically relevant to busulfan CL. We did not suggest the guidance of *GSTA1* genotype on initial busulfan dose in Chinese adult patients.

Keywords Busulfan · Adult · *GSTA1* · Polymorphism · Population pharmacokinetic

Introduction

High-dose busulfan is commonly used as the cornerstone of chemotherapy regimen prior to hematopoietic stem cell transplantation (HSCT) [1]. Targeted busulfan is necessary because of the definite dosage–response relationship and narrow therapeutic index: subtherapeutic busulfan systemic exposure, expressed as area under the curve (AUC) < 900 μmol × min/L, results in relapse or graft failure, while supratherapeutic AUC > 1500 μmol × min/L, is associated with fatal toxicities, such as hepatic veno-occlusive disease (VOD) [2, 3]. Since very few busulfan AUCs achieve the therapeutic range after their initial standard doses [4, 5], an individualized busulfan initial dose is warranted for the targeted AUCs to improve clinical efficiency.

Yidan Sun and Jingjing Huang contributed equally to this work.

Electronic supplementary material The online version of this article (https://doi.org/10.1007/s00280-019-04001-2) contains supplementary material, which is available to authorized users.

✉ Jiong Hu
hujiong@medmail.com.cn

[1] Department of Bone Marrow Transplantation, Ruijin Hospital, Shanghai Jiao Tong University School of Medicine, No.197 Ruijin Er Road, Shanghai 20025, China

[2] Department of Pharmacy, Ruijin Hospital, Shanghai Jiaotong University School of Medicine, Shanghai, China

[3] Shanghai Jiaotong University School of Medicine, Shanghai, China

[4] NeoTrident Co. Ltd., Beijing, China

Noteworthily, studies [6–8] showed that glutathione S-transferase (GST) genotypes played a positive role in the individualization of busulfan dose for optimal clinical outcomes. GSTs, which are the enzymatic superfamily of detoxification, catalyze the conjugation of busulfan with glutathione (GSH) in liver [9]. Of all, GSTA1 is the predominant GST isoenzyme of busulfan metabolism, with minor contributions by GSTM1 and GSTP1 in vitro studies [10]. *GST* polymorphisms, gene deletion or single nucleotide polymorphism (SNP), cause a decreased metabolic activity of busulfan in patients with genetic variants [11]. In pediatric patients, Nava et al. [6] showed that *GSTA1* diplotypes linked to poor busulfan metabolism and associated with AUCs within the toxic range. Consistently, *GSTA1* diplotypes influenced the prediction errors of the weight- and age-based methods which are used to calculate the initial doses of busulfan. However, busulfan initial dosing guided by *GST* genotypes is not recommended in clinical practice due to inconsistent effect of the genetic polymorphism on the pharmacokinetic, efficacy, or toxicity of busulfan [12]. Studies about the influence of *GST* polymorphisms on busulfan pharmacokinetic (PK) are scant in Asian patients. The PK study of Yin et al. [8] demonstrated that *GSTA1* and *GSTP1* polymorphisms are significantly associated with busulfan exposure in Chinese adult patients. In addition, both Yin et al. [8] and our previous study [13] showed low busulfan exposure after the first dose in the Chinese population. We found that about half of the first AUCs were below the therapeutic range. These are a necessity to personalize the initial dose of busulfan to improve clinical outcome in Chinese patients.

This study aimed to quantify the impact of *GSTA1, GSTP1,* and *GSTM1* genotypes on busulfan PK variability by population pharmacokinetic (PPK) analysis, and to clarify the role of genetic factors on the individualization of busulfan initial dose in Chinese adult patients undergoing HSCT.

Materials and methods

Patients

Forty-three adult patients who underwent HSCT for malignant diseases were enrolled in the modeling group at the department of Blood Marrow transplantation of Ruijin Hospital, Shanghai, China, from May 2011 to October 2014. Nineteen adult patients were enrolled in the validation group from March 2017 to August 2017. All procedures performed in this study were approved by the Ruijin Hospital Research Ethics Committee and in accordance with the 1964 Helsinki Declaration. Before the study, informed consent was obtained from the enrolled patients.

All patients received intravenous busulfan (Busulfex; Kyowa Hakko Kirin Co., Ltd, Tokyo, Japan) at 1.6 mg/kg twice daily. Busulfan was given as part of the BUCY, BUFLU, and CBV regimens. For BUCY regimen, busulfan was given over 2 h for 4 days on days − 8 to − 5 followed by intravenous cyclophosphamide (CY) 60 mg/kg once daily on days − 3 and − 2. For BUFLU regimen, intravenous fludarabine (FLU) 30 mg/m^2 was given once daily with busulfan on day − 6 and − 3. The CBV regimen in validation group included 3 days of busulfan from day − 8 to − 6, VP16 at 400 mg/m^2 daily on day − 5 and − 4 and CY 50 mg/kg daily on day − 3 and − 2. Then, gemcitabine was given at 75 mg/m^2 on day − 9 and at 10 mg/m^2 on day − 5, respectively.

Blood sampling and analysis

Blood samples were collected before busulfan infusion and at 0.5 h, 1 h, 1.5 h, 2 h, 2.5 h, 3 h, 4 h, 5 h, 6 h, 8 h, and 10 h after starting the first dosing. All the blood samples were drawn from a peripheral vein in the arm opposite to the central line where busulfan was infused. 3 mL of whole blood sample was collected in EDTA anticoagulant glass tubes. 1 ml of whole blood for DNA extraction was taken from the samples obtained before busulfan infusion. The residual whole blood was centrifuged at 3000 rpm for 10 min at 4 °C for plasma separation. Busulfan plasma concentrations were analyzed using a validated analytical method [13] by liquid chromatography–electrospray–tandem mass spectrometry. High-performance liquid chromatography separations were performed on an Agilent Eclipse XDB-C18 analytical column (100 mm × 2.1 mm, 3.5 μm) with a column temperature of 40 °C. The plasma was eluted using a mobile phase composed of 2 mmol/L ammonium formate solution (0.1% formic acid)-acetonitrile (60:40, V/V) at a flow rate of 0.2 mL/min. Electrospray ionization mass spectrometry was performed in multiple reaction monitoring mode with the target ions m/z 264.2 → 151.1 (busulfan) and m/z 278.3 → 69.2. The linearity range of busulfan standard curve was 25–2500 ng/mL ($R = 0.999$). The intraday and inter-day accuracies of busulfan quality control samples were from 96.4 to 109.2% and from 99.2 to 111.2%, respectively. The extraction recovery of busulfan was from 102.0 to 113.7%.

DNA extraction and glutathione S-transferases genotyping

The whole blood samples for DNA extraction were obtained before HSCT. DNA was extracted from peripheral blood lymphocytes by TIANamp Blood DNA Kit (Tiangen Biotech Co., Ltd, Beijing, China). The following genetic variants were determined: *GSTA1* -69 C/T (rs3957357), *GSTP1* 313A/G (rs1695), *GSTM1* (null allele). The *GSTA1* haplotype (*GSTA1*A* and *GSTA1*B*) was determined by the -69

C/T variation in the prompter region of *GSTA1*. This SNP was previously shown in complete linkage disequilibrium with -631T/G, -567T/G, and -52G/A [14]. The SNPs in the *GSTA1* and *GSTP1* genes were genotyped by SNaPshot assay according to the manufacturer's protocols (ABI SNaPshot Multiplex kit, CA, USA). The promoter region of the *GSTA1* gene was amplified with the forward primer GSTA1-F (5′-GCTCGACAACTGAATTCCAGGTC-3′) and the reverse primer GSTA1-R (5′-CCCTAGTCTTTG CACCCAACTCAT-3′). The promoter region of the *GSTP1* gene was amplified with the forward primer GSTP1-F (5′-CTCATCCTTCCACGCACATCCT-3′) and the reverse primer GSTP1-R (5′-TTTCTTTGTTCAGCCCCCAGTG-3′). Analysis was carried out using Genemapper software (version 4.1; Life Technologies). The *GSTM1* gene was PCR amplified (215 bp) together with albumin gene (268 bp) as an internal control [15]. The primer pairs were as follows: GSTM1-F, 5′-GAA CTC CCT GAA AAG CTA AAG C-3′ and GSTM1-R, 5′-GTT GGG CTC AAA TAT ACG GTG G-3′, which yield a 215 bp fragment and β-actin-F, 5′- CAA CTTCAT CCA CGT TCA CC-3′ and β-actin-R, 5′- GAA GAG CCAAGG ACA GGT AC-3′, which yield a 268 bp fragment. PCR products were analyzed on a 2% agarose gel.

Development of a population pharmacokinetic model

A PPK model was developed by nonlinear mixed-effect modeling using Phoenix NLME software, Version 1.4 (Pharsight, A Certara Company, USA), according to the best practices and guidance [16]. The first-order conditional estimation method with extended least squares method (FOCE ELS) was adopted in the whole process to estimate PK parameters and their variability.

Structure model

Plasma concentration data were natural logarithm transformed before PPK modeling. Initially, a one-compartment model with first-order elimination was used as the base model, according to our previous study [13]. The model was parameterized in terms of total body clearance (CL) and volume of distribution (V_d). The inter-individual variability of the PK parameters was estimated using an exponential error model, where P_i represents the individual parameter estimate, P is the typical parameter estimate, and η_i is the unexplained inter-individual variability, which is assumed to follow a normal distribution with a mean of 0 and variance ω^2:

$$P_i = P \times e^{\eta i}.$$

A residual variability (additive, proportional, exponential and mixed random intra-individual residual error) model was explored to account for the intra-individual variability according to the log-likelihood (LL) difference between models [the improvement of objective function value (OFV)].

Covariate analysis

The effects of age, sex, actual body weight, body surface area (BSA), diagnoses, hepatic function markers [alanine transaminase (ALT), aspartate aminotransferase (AST), alkaline phosphatase (ALP), total bilirubin (TBI)], *GST* genotypes, and conditioning regimen on pharmacokinetic parameters were investigated as potential covariates . The effects of continuous covariates were modeled in a linear or nonlinear relationship using the following equations:

$$P_i = tv(\mathrm{P}) + \theta \times (\text{covariate/typical value})$$
$$P_i = tv(\mathrm{P}) + \theta \times (\text{covariate} - \text{typical value})$$
$$P_i = tv(\mathrm{P}) \times (\text{covariate/typical value})^{\theta}$$

where tv (P) is the typical value of P, P_i is the value of P for individual, and θ is the estimated effect of the covariate on P.

For categorical covariates, the effect on P was modeled using the following equation:

$$P_i = tv(P)\text{Indicator} = 0$$
$$P_i = tv(P) \times \theta\text{Indicator} = 1$$

where indicator represents the binary covariate being assigned to 0 or 1.

The stepwise covariate modeling and likelihood ratio test were used to test the effect of each variable. The selection of covariates was initially selected by data visualization and biological plausibility. Further screening of potential covariates was performed by forward addition ($P < 0.05$) and backward elimination ($P < 0.01$) based on the changes in OFV: any decreases in OFV by more 3.84 and 6.63 (1 degree of freedom) denote an improved fit at $P < 0.05$ and $P < 0.01$, respectively. An additional criterion for covariate retention was reduction in the inter-individual variability and improvement in the parameter estimate precision. Clinical significance was also considered for retention of a potential covariate.

Model validation

Accuracy and stability of prediction of the final covariate model were validated both internally and externally.

Graphical inspection of the final model adopted goodness-of-fit plots, including observed concentrations (OBS) versus population predicted concentrations (PRED), OBS

versus individual predicted concentrations (IPRED), conditional weighted residuals (CWRES) versus PRED, and CWRES versus time after the first dose. The CWRES results were summarized graphically using the quantile–quantile (Q–Q) plot and the histogram. Bootstrap analysis was performed for internal validation of model. 1000 resamples from the original data were performed. Mean values and 95% confidence interval (CI) of bootstrap parameters were compared with estimates of the final model. The final model was also evaluated graphically and statistically by visual predictive checks (VPC). The final model parameters were used to simulate a data set for 200 replicates and the 5th and 95th CIs of simulated values were processed for VPC.

To validate the developed model externally, the model was further evaluated in an independent group of adult patients undergoing HSCT. The individual PK parameters were predicted by Bayesian estimation (MAXEVAL = 0 in the estimation step, where MAXEVAL is the maximum number of model evaluations that can be used) with Phoenix NLME using the parameters of the final model. The predictive performance was evaluated by calculating the prediction error (PE) and absolute prediction error (APE) using the following equations:

$$\mathrm{PE\%} = (\text{Bayesian simulated} - \text{Observed})/\text{Observed}$$

$$\mathrm{APE\%} = |\text{Bayesian simulated} - \text{Observed}|/\text{Observed}$$

Statistical analysis

The continuous variables were represented as mean with standard deviation or 95% CI. Statistical significance of the difference between groups was calculated by Chi square test. P values < 0.05 were considered significant.

Results

Patients' characteristics and *GST* genetic frequencies

The mean age of patients was 31.5 years, and 74.4% of them were male. The mean weight was 64.3 kg in the modeling group ($n = 43$). There were 19 enrolled patients in the validation group. The age, sex, and weight were not significantly different ($P > 0.05$) between the validation group and modeling group. Patients' characteristics are presented in Table 1. Most of the enrolled patients received allogenous HSCT from a human leukocyte antigen-matched donor using peripheral blood stem cells for their hematological malignancies. Five patients in the validation group received autologous HSCT.

The *GST* genetic frequencies are shown in Table 2. 10 of 43 (23.2%) patients were heterozygous genotype of *GSTA1* (*GSTA1*A*B*), and only 1 patient (2.4%) was homozygous *GSTA1* (*GSTA1*B*B*). Genetic frequency of *GST A1**B haplotype was 14.0%. Both *GSTA1* and *GSTP1* genetic frequencies of patients in modeling group were in Hardy–Weinberg equilibrium (HWE). 2 of the 19 patients in validation group were heterozygous and homozygous *GSTA1*B*, respectively. The *GSTA1* genetic frequency was not in HWE.

Structure model

A total of 488 busulfan concentrations from 43 patients were obtained for model development. A one-compartment model with first-order elimination best described the PK of intravenous busulfan. The intra-individual variability of the plasma concentration was estimated using the proportional error model finally. The estimated CL and Vd of basic model were 14.2L/h and 64.1L, respectively.

Covariate analysis

Age, actual body weight, body surface area, and hepatic function markers (ALT, AST, ALP, TBI) were tested as continuous covariates. Sex, diagnoses, *GST* genotypes, and conditioning regimen were tested as categorical covariates, while non-Hodgkin's lymphoma, myelodysplastic syndromes, and hybrid acute leukemia patients were analyzed together with acute lymphoblastic leukemia patients relative to the patients with acute myelocytic leukemia and chronic myelocytic leukemia due to their small number. The patients with *GSTA1*B*B* or *GSTP1*G*G* were excluded to avoid statistical deviation.

GSTA1 genotype was a covariate on busulfan CL in a statistically significant manner. OFV decreased by 15.64 from 4942.75 (basic model) to 4927.11 (final model), adding the covariate of *GSTA1* genotype. The individualized CL was estimated by the following equation:

$$\mathrm{CL} = tv\,\mathrm{CL} \times \left(1 + \mathrm{CL}_{\mathrm{part}} \times G_{GSTA1}\right) \times e^{\eta_{\mathrm{ij}}},$$

where $G_{GSTA1} = 1$ for *GSTA1*A*B*, 0 for *GSTA1*A*A*. Population-estimated CL of the final model was 15.0 L/h for a typical patient with *GSTA1*A*A* wild type. The inter-individual variability of CL declined from 17.8 to 16.8%, after inclusion of *GSTA1* genotype as a covariate. The estimated PPK parameters and bootstrap results are listed in Table 3.

Model evaluation

Goodness-of-fit plots of the final model in Fig. 1 showed that the PRED and IPRED were in reasonable agreement with OBS. Distribution of CWRES versus predicted concentration and time after dose were shown to be close to zero and uniformly distributed within the range (− 2 to 2) in the final

Table 1 Characteristics of patients in the modeling group and validation groups

Characteristic	Modeling group ($n=43$)	Validation group ($n=19$)	
Age, years, mean (SD)	31.5 (10.6)	35.4 (10.9)	
Sex (male), *n* %	32 (74.4)	12 (63.2)	
Weight, kg, mean (SD)	64.3 (13.1)	65.5 (7.31)	
Height, cm, mean (SD)	171.8 (13.1)	169.1 (8.07)	
BSA, m^2, mean (SD)	1.80 (0.274)	1.73 (0.147)	
BMI classification (kg/m^2), *n*			
Normal (range 18.5–24.9)	33	15	
Overweight (range 25.0–29.9)	10	4	
Diagnosis, *n* %			
AML	19 (44.2)	AML	3 (15.8)
ALL	12 (27.9)	ALL	3 (15.8)
CML	4 (9.3)	CML	1 (5.3)
NHL	5 (11.6)	CLL	1 (5.3)
MDS	2 (4.6)	NHL	5 (26.3)
HAL	1 (2.4)	MDS	4 (21.0)
		HL	2 (10.5)
Type of donor, *n* %			
MS-allo-HSCT	30	MS-allo-HSCT	11
MUD-allo-HSCT	13	MUD-allo-HSCT	3
		Auto-HSCT	5
Conditioning regimen, *n* %			
Busulfan-cyclophosphamide	22 (51.2)	CBV + gemcitabine	5 (26.3)
Busulfan-fludarabine-ATG	21 (48.8)	Busulfan-fludarabine-ATG	14 (73.7)

ALL acute lymphoblastic leukemia, *Allo* allogenous, *AML* acute myelocytic leukemia, *ATG* antithymocyte globulin, *Auo* autologous, *BMI* body mass index according to National Heart, Lung, and Blood Institute weight categories, *CLL* chronic lymphoblastic leukemia, *CML* chronic myelocytic leukemia, *HAL* hybrid acute leukemia, *HL* Hodgkin's lymphoma, *HSCT* hematopoietic stem cell transplantation, *MDS* myelodysplastic syndromes, *NHL* non-Hodgkin's lymphoma, *MS* matched sibling, *MUD* matched unrelated donor

Table 2 *GST* genetic frequencies of modeling group and validation group

SNP	Genotype	Frequency (%)
Modeling group ($n=43$)		
GSTA1-69C/T (rs3957357)	CC	32 (74.4%)
	CT	10 (23.2%)
	TT	1 (2.4%)
GSTP1313A/G (rs1695)	AA	30 (69.8%)
	AG	12 (27.9%)
	GG	1 (2.3%)
GSTM1 deletion	Positive	23 (53.5%)
	Null	20 (46.5%)
Validation group ($n=19$)		
GSTA1-69C/T (rs3957357)	CC	17 (89.4%)*
	CT	1 (5.3%)
	TT	1 (5.3%)

*$P=0.005$ from Hardy–Weinberg equilibrium test

model. Additionally, the CWRES distribution and histogram indicated that the assumption of normal distribution of the differences between PRED and OBS was acceptable, as shown in Figure S1. The robustness of the final model was internally validated by the bootstrap results. The population-estimated parameters were similar to the simulation values and within 95% CI from bootstrap analysis, as shown in Table 3. The VPC in Fig. 2 showed that the observed values were almost all positioned within the 5th and 95th CIs of simulated values. The results demonstrated the accuracy of the final model.

Busulfan concentrations from 19 patients in the external validation group were used to validate the final *GSTA1* genotype-based model. The predictive performance of the final PPK model was evaluated by the comparison between the observed values (CL_{obs} and AUC_{obs}) and the simulated values (CL_{sim} and AUC_{sim}),as shown in Fig. 3. The Bayesian simulated PK parameters highly correlated with the observed data ($r^2=0.98$ for the CL_{obs} with CL_{sim} and $r^2=0.84$ for the AUC_{obs} with AUC_{sim}). The mean PE (MPE, %) and mean APE (MAPE, %) of the CL_{sim} were 4.04% (95%CI: 4.02% to 4.06%) and 4.39% (95% CI: 4.57% to 4.51%). The MPE

Table 3 Population pharmacokinetic parameters of intravenous busulfan and bootstrap results

Parameter	Base model	Final model	Bootstrap ($n = 1000$)	
			Mean	95% CI
Pharmacokinetic parameter				
V (L)	64.1	64.1	64.1	(60.7 to 67.5)
CL (L/h)	14.2	15.0	15.0	(14.0 to 15.9)
CL_{part}		− 0.214	− 0.215	(− 0.282 to − 0.127)
Inter-individual variability				
ωV (%)	16.7	14.6	14.5	(14.2 to 14.9)
ωCL (%)	17.8	16.7	16.7	(15.9 to 17.1)
Residual variability				
Proportional σ (%)	− 14.2	− 14.1	− 14.2	(− 16.1 to − 12.1)

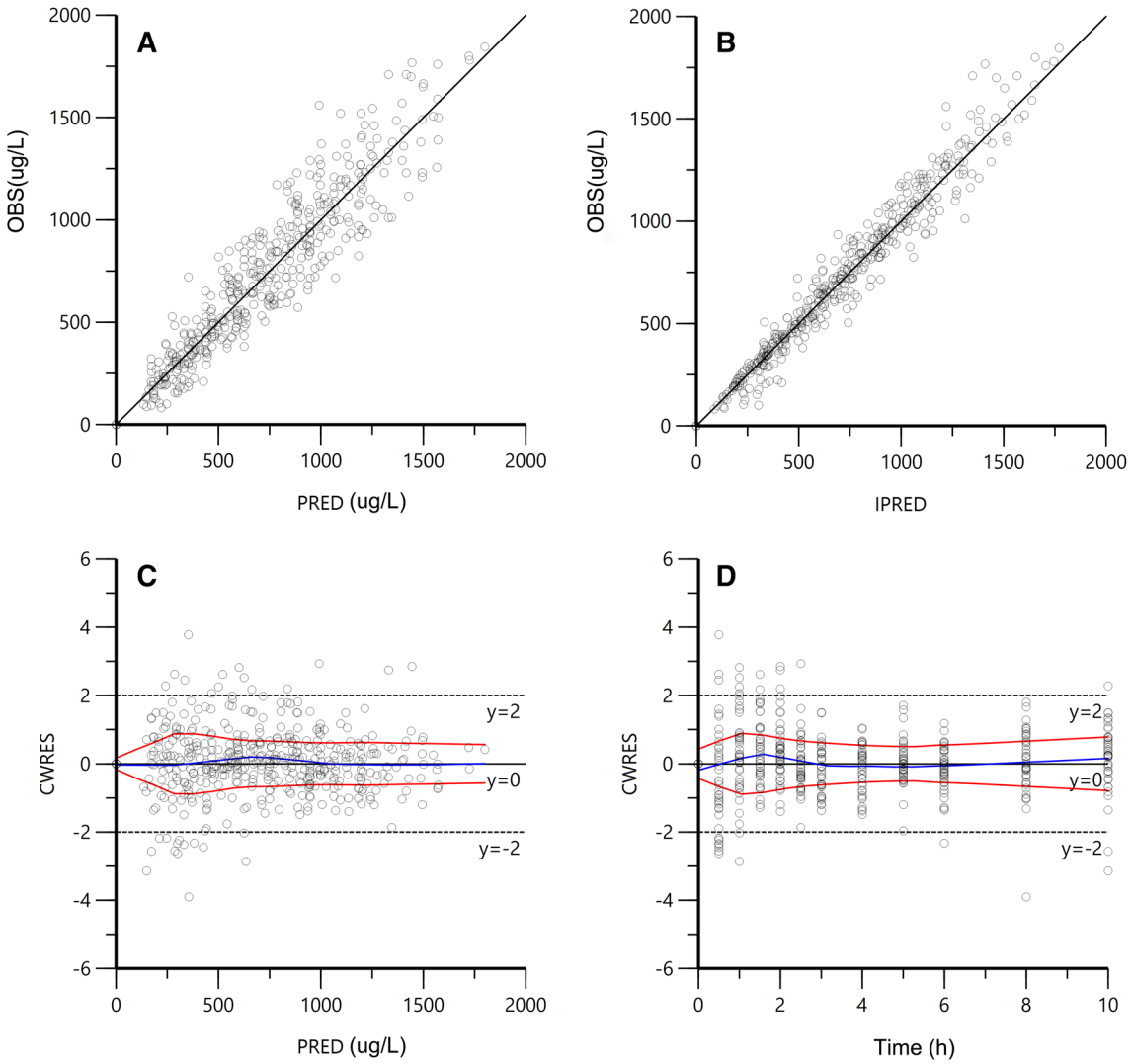

Fig. 1 Goodness-of-fit plots of the final model. **a** Observed concentrations versus population predicted concentrations; **b** observed concentrations versus individual predicted concentrations; **c** conditional weighted residuals versus population predicted concentrations; **d** conditional weighted residuals versus time after the first dose. OBS means observed concentration; PRED means population predicted concentrations; IPRED means individual predicted (IPRED) concentrations; CWRES means conditional weighted residuals

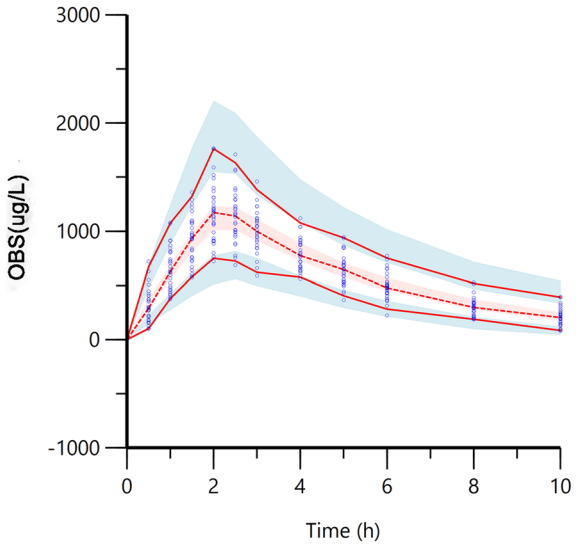

Fig. 2 The visual predictive check (VPC, $n = 1000$) of final model. The dots represent observed concentrations. The lines represent observed concentrations and the shadow represents the 5th and 95th percentiles of the simulated values

and MAPE of the AUC_{sim} were − 2.55% (95%CI: − 2.58% to − 2.52%) and 4.93% (95%CI: 4.92% to 4.94%).

Discussion

In this study, we developed the PPK model of intravenous busulfan, incorporating *GST A1* genotype, and externally validated the accuracy and stability of the model in Chinese adult patients undergoing HSCT. The estimated CL of intravenous busulfan was 14.2 L/h (3.64 mL/min per kg) and consistent with the CL of 4.02 mL/min per kg in another study [8] of Chinese adult patients, higher than 1.9 mL/min per kg and 3.34 mL/min per kg in Caucasian patients [17, 18]. Inclusion of *GSTA1* genotype as a covariate accounted for 1.1% of the inter-individual variability of busulfan CL in the final model.

The fast metabolism of busulfan might relate with the ethnic difference of *GSTA1* genotype between Chinese patients and Caucasian patients. The patients with *GST A1*B* haplotype were the poorer metabolizers with lower CL of busulfan compared to those with wild type. The studies of Kusama et al. [19] and Kim et al. [20] showed significant impact of *GST A1* genotype on busulfan CL. Genetic frequency of *GST A1**B haplotype was 14.0% with 1 patient of homozygous excluded to avoid statistic deviation in our study. The distribution was consistent with the rarity of haplotype **B* in the Asian population (42.9% versus 13.9% in the Caucasians and Asians) [21]. *GSTA1*-69C/T (rs3957357), with -631T/G, -567 T/G, and -52 G/A, is located in the promoter region of *GSTA1* gene. *GSTA1*-69C/T can adequately identify *GSTA1**B haplotype which showed significant decline of GSTA1 protein expression in vitro [22]. Ansari et al. [23] further distinguished **B 1b*, **B 1a* and **B* 2 haplotypes by − 513 (rs11964968), − 1142 (rs58912740). Then, Nava et al. [6] classified **A*B* and **B*B* diplotypes into normal and poor metabolizers of busulfan. Based on this accurate *GSTA1*-genotype classification, the PPK model excellently predicted the initial busulfan doses and achieved the target AUC in 85.2% of the pediatric patients (95%CI 78.7–91.7%) [7]. However, this metabolic classification of busulfan was not appropriate for Chinese patients due to the low genetic frequencies of above *GSTA1*B* variants in the Asian population [21].

PPK analysis has shown an advantage of quantifying the effects of covariates on PK variability to assess the clinical relevance of those effects [24]. Our results showed that *GSTA1* genotype explained a tiny part of inter-individual variability from 17.8% of the basic model to 16.7% of the final model. The low genetic frequency of *GST A1*B* may lead to minimal influence of *GSTA1* genotype and limited

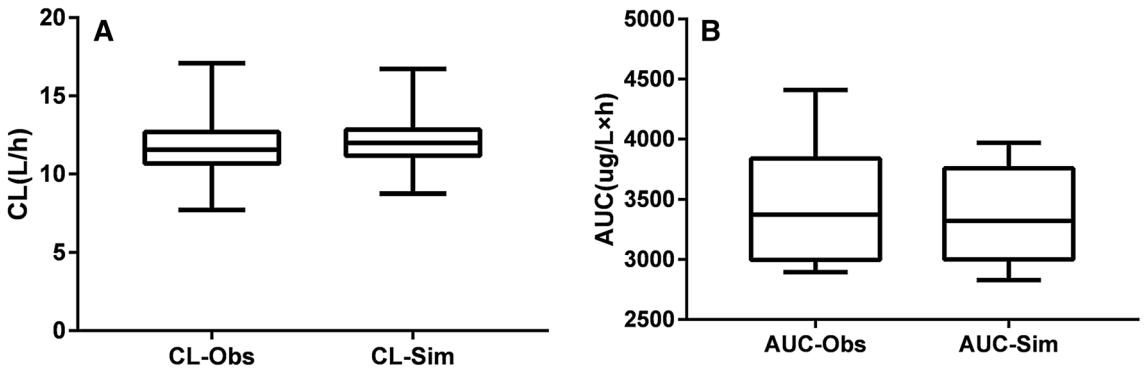

Fig. 3 *GSTA1* genotype-based simulations of CL and AUC in validation group ($n = 19$). **a** The box and whisker plot of observed CL and simulated CL. **b** The box and whisker plot of observed AUC and simulated AUC

Table 4 Pharmacogenomics data about busulfan pharmacokinetics in the patients undergoing hematopoietic stem cell transplantation

No.	Administration	Population	Conditioning	Involved genetic polymorphisms	Conclusions	Results	References
1	N/A	Adults; Japanese; $n=55$	BUCY	*GSTM1*, *GSTT1*, *CYP2B6*, *CYP2C9*, *CYP2C19*	*GSTA1*A/*A* genotype for lower BU first dose AUC (AUC_{1st})	*GSTA1* polymorphism was significantly associated with AUC_{1st} [coefficient, 1897.9 μg × h/L, 95% CI (891.9–2903.9 μg × h/L), $P=0.0004$]	Terakura et al. [31]
2	Oral	Adults; Canadians; $n=119$	N/A	*GSTA1*	*GSTA1*B* for lower BU oral CL (CL_O)	Carriers of *GSTA1*B* exhibited lower BU CL_O than patients with an **A/*A* genotype ($P<0.002$): BU CL was 166 ± 31, 187 ± 37 vs. 207 ± 47 mL/min for *GSTA1*B/*B*, **A/*B* and **A/*A* genotypes, respectively	Michaud et al. [32]
3	Intravenous	Children; Japanese; $n=20$	N/A	*GSTA1, GSTM1, GSTT1*	Not found	*GSTA1*, *M1*, and *T1* independently showed no significant differences in $AUC_{0-\infty}$, CL, and elimination rate constant	Nishikawa et al. [33]
4	Intravenous	Children and adolescents; Canadians; $n=112$	Mixed	*GSTA1*	*GSTA1* diplotypes for BU CL	Compared to *GSTA1* normal metabolizers, rapid metabolizers had 7% faster CL rates, while poor metabolizers had 12% slower CL rates	Nava et al. [7]
5	N/A	Children; Caucasians; $n=138$	N/A	*GSTA1*, *GSTP1*, *GSTM1*	*GSTA1* diplotypes for BU CL	*GST A1* diplotypes underlying fast and slow metabolisms showed higher and lower BU CL ($P=0.009$)	Ansari et al. [25]
6	Intravenous	Children; Italians; $n=44$	BUCY	*GSTA1*, *GSTM1*	*GSTA1*B* for higher BU exposure and lower CL	Individuals with the *TT − 69* genotype (or **B*B* haplotype) had significantly higher first Bu C_{ss} compared to individuals with the *CC* genotype (or **A*A* haplotype combination). Consequently, CL decreased and was slowest in *TT* individuals	Ansari et al. [26]

Table 4 (continued)

7	Intravenous	Adults; Korean; $n=36$	BUCY or BUFLU	*GSTA1, GSTP1, GSTM1, GSTT1*	*GSTA1* variants decreased BU CL and increased exposure	CL decreased by 15% and AUCs increased with *GSTA1* variants compared with wild type (both $P<0.05$)	Choi et al. [31]
8	Intravenous	Adults; Chinese; $n=25$	BUCY	*GSTA1, GSTP1*	*GSTA1* and *GSTP1* variants for high BU exposure and low CL	The *GSTA1 *A/*B* genotype group showed a significantly higher AUC ($P<0.0001$), higher C_{max} ($P=0.0003$) and lower CL ($P=0.0007$) than the *GSTA1 *A/*A* genotype group. AUC was lower in *GSTP1 *A/*A* genotypes compared with**A/*G* ($P=0.0283$) and **G/*G* genotypes ($P=0.0111$). The BU CL in *GSTP1 *A/*A* genotype was shown to be higher than **A/*G* ($P=0.0255$) and *G/*G genotypes ($P=0.0111$)	Yin et al. [8]
9	Intravenous	Adults; Dutch; $n=65$	BUCY or BUFLU	*ABCB1*, *ABCB4*, *ABCC2*, *ABCC6*, *CYP2B6*, *CYP39A1*, *CYP3A7*, *CYP4F2*, *FMO1*, *GSTA1*, *GSTA5*, *NR3C1*, *PPARD*, *UGT2B15*	*GSTA5* affected BU CL	*GSTA5* (rs4715354 and rs7746993) remained significantly associated with BU CL ($P=0.025$)	Ten Brink et al. [35]
10	Intravenous	Children; Dutch; $n=84$	BUCY or BUFLU	*GSTA1*, *CYP2C19*, *CYP39A1*, *ABCB4*, *SLC22A4*, *SLC7A8*	*GSTA1* and *CYP39A1* for BU CL	*GSTA1* (rs3957357; $P=0.004$) and *CYP39A1* (rs9381468 and rs953062; $P=0.011$) were associated with BU CL: explained17% of the variability in BU CL. Furthermore, the effect of *GSTA1* haplotype on CL was dependent on age	Ten Brink et al. [36]

Table 4 (continued)

11	Intravenous	Children; Canadians; $n=44$	BUCY-based or BU/Melphalan	*CYP2C9*, *CYP2C19*, *FMO3*, *CYP2B6*	*CYP2C9* has a role in BU metabolism	The ratio of BU to sulfolane (water-soluble metabolite of BU) was considered the metabolic ratio (MR); higher MRs were observed in *CYP2C9*2* and **3* allele carriers (7.8 ± 3.6 in carriers vs 4.4 ± 2.2 in noncarriers; $P=0.003$)	Uppugunduri et al. [37]
12	Intravenous	Adults; Italians; $n=185$	BUCY or BUFLU	27 loci were analyzed	*GSTA2 S112T* for BU AUC	*GSTA2 S112T* serine allele homozygosity predicts a wider BU AUC (1214.36 ± 570.06 versus 838.10 ± 282.40 μmol × min/L)	Bonifazi et al. [38]
13	Oral	Adults; Israelites; $n=63$	BUCY	*GSTP1*, *GSTA1*, *GSTM1*, *GSTT1*, *ABCB1*	AML patients with the *GSTP1* rs1695 variant allele and *GSTM1-ABCB1* for CL and AUC	*GSTP1* rs1695 variant allele (*G*) was associated with reduced BU CL ($P<0.03$), as was *ABCB1* rs2032582 ancestral (*G*) allele (*2677*) ($P<0.05$); *GSTP1*(*A/A*) variant allele for the increased BU CL ($P<0.05$). *GSTM-positive*, having two ancestral *ABCB1 3435C* alleles correlated with increased BU CL ($P<0.05$) and decreased AUC ($P<0.05$). In *GSTM1-null* patients, carriers of two ancestral *3435C* alleles displayed lower CL ($P<0.05$) and higher AUC ($P<0.05$) compared to carriers of the *variant 3435T* allele	Krivoy et al. [38]

Table 4 (continued)

14	Intravenous	Adults; Dutch; $n=66$	BUFLU or BU-alemtuzumab	*GSTA1*, *GSTP1*, *GSTM1*	*GSTA1 *A/*A* for a high BU CL	A higher clearance was observed in the *GSTA1 *A/*A* genotype group (0.21 ± 0.055 L/h/kg) compared with *GSTA1*B* heterozygous patients (0.18 ± 0.041 L/h/kg) and *GSTA1*B* homozygous patients (0.15 ± 0.039 L/h/kg)	ten Brink et al. [39]
15	Intravenous	Adults; Dutch; $n=66$	BUCY or BUFLU or BU	*GSTA1*, *GSTM1*, *GSTT1*	*GSTA1*B* and *GSTM1/GSTT1-null* for low CL	Carriers of *GSTA1*B* showed significantly lower BU CL than *GSTA1*A/*A* carriers ($P=0.015$). *GSTM1/GSTT1-null* genotype was significantly associated with BU CL ($P=0.048$)	Kim et al. [20]
16	Oral	Children; Dutch; $n=18$	BUCY	*GSTA1*, *GSTP1*, *GSTM1*, *GSTT1*	*GSTA1* and *GSTP1* for C_{max}, AUC, and CL; *GSTM1-null* for lower BUAUC	*GSTA1* and *GSTP1* genotypes associated with BU C_{max} ($P=0.01$, $P=0.02$), AUC ($P=0.02$, $P=0.01$) and BU CL ($P<0.02$, $P=0.08$). *GSTM1-null* individuals had the lowest C_{max}/AUC ratio ($P<0.001$)	Elhasid et al. [40]
17	Intravenous	Children; Canadians; $n=28$	BUCY	*GSTA1*, *GSTP1*, *GSTM1*	*GSTM1-null* for high C_{max}, AUC, C_{ss}, and low CL	*GSTM1-null* individuals had higher drug exposure ($P_{Cmax}=0.008$; $P_{AUC}=0.003$; $P_{Css}=0.02$) and lower CL ($P_{CL}=0.001$)	Ansari et al. [23]

Table 4 (continued)

18	Oral	Adults; Japanese; $n=12$	N/A	*GSTA1*	*GSTA1*A/*B* for low CL and high concentration	*GSTA1*A/*B* group had significantly lower elimination constant (0.176 ± 0.038 vs. 0.315 ± 0.02 L/h; $P=0.008$) and CL corrected by bioavailability (0.118 ± 0.013 vs. 0.196 ± 0.011 L/h/kg; $P=0.004$), and significantly higher mean plasma busulfan concentration (1344 ± 158 vs. 854 ± 44 ng/ml; $P=0.001$) than the wild type	Kusama et al. [19]
19	Intravenous and oral	19 studies	N/A	*GSTA1*, *GSTP1*, *GSTM1*	*GSTA1*B* and *GSTM1 null* genotypes decreased CL_{IV}, *GSTA1*B* increased AUC_{IV}	*GSTA1*B* and *GSTM1 null* genotypes decreased CL_{IV} of BU [standardized difference in means (SDM) $=-1.103$; $P=0.019$ and SDM $=-0.418$; $P=0.002$, respectively]. *GSTA1*B* increased AUC_{IV} of BU (SDM $=0.832$; $P=0.046$), whereas *GSTM1* did not (SDM $=0.155$; $P=0.478$)	Kim et al. [41]
20	Intravenous	Children; Caucasian; $n=148$	N/A	*GSTA1*	*GSTA1*diplotypes affect BU AUC	*GSTA1* diplotypes linked to poor BU metabolism (G3) associated with AUC within target (OR: 4.7, 95% CI: 1.1–19.8, $P=0.04$); G3 was associated with AUCs within the therapeutic and the toxic range, whereas rapid metabolizers (G1) were correlated with subtherapeutic AUCs	Nava et al. [6]

Table 4 (continued)

21	Oral	Children; French; $n=114$	BUCY	*GSTM1*, *GSTT1*	*GSTM1-null* genotype for high CL/F and low C_{ss}	The patients with the *GSTM1-null* genotype showed significantly higher Cl/F ($P=0.00001$) and lower C_{ss} of BU ($P=0.001$) after the first dose compared with those with the *GSTM1-positive* genotype	Srivastava et al. [42]
22	Oral	Adults; Norwegians; $n=114$	BUCY	*GSTA1*, *GSTP1*, *GSTM1*, *GSTT1*	*GSTA1*B* allele for higher BU C_{ss}	Median first dose BU C_{ss} was 1000 mcg/L (600–1780 mcg/L). Patients carrying 1 and 2 *GSTA1*B* (rs3957357) alleles demonstrated median 12% and 16% higher BU C_{ss} ($P \leq 0.05$)	Bremer et al. [43]
23	Intravenous	Children; Canadians; $n=69$	BUCY	*GSTA1*, *GSTP1*, *GSTM1*	*GSTM1* null genotype for high BU exposure and low CL; *GSTA1*A2* haplotype for low drug levels and high CL	*GSTM1* null genotype correlated with higher BU exposure and lower CL in patients older than 4 years ($P \leq 0.04$). *GSTA1*A2* haplotype was associated with lower drug levels and higher drug clearance ($P \leq 0.03$)	Ansari et al. [44]
24	Intravenous and oral	Adults; Americans; $n=57$ (intravenous); $n=95$ (oral)	N/A	*GSTA1*, *GSTM1*	*GSTA1*A* allele for higher oral Bu CL	Oral BU CL was associated with *GSTA1* ($P=0.008$). Those patients with the *GSTA1*A*A* haplotype and *GSTA1*A*B* genotype had an oral BU CL that was 0.45 mL/min/kg (16%) higher and 0.41 mL/min/kg (14%) than those with *GSTA1*B*B* genotype. CL of IV BU was not associated with *GSTA1* ($P=0.21$)	Abbasi et al. [28]

Table 4 (continued)

25	Intravenous	Children; Dutch; $n=77$	BU with CY, FLU, or other combinations	*GSTA1*, *GSTM1*, *GSTP1*, *GSTT1*	NOT found	None of the studied polymorphisms in the genes encoding *GSTA1* *GSTM1*, *GSTP1*, and *GSTT1* nor combinations of genotypes were significant covariates	Zwaveling et al. [45]
26	Intravenous	Children; Dutch; $n=29$	BUCY or BUFLU	*GSTA1*, *GSTM1*, *GSTP1*	*GSTA1*B* allele for the reduced BU CL	Carriers of *GSTA1*B* had a 2.6-fold higher BU AUC and C_{ss} compared with noncarriers ($P \leq .01$). Carriers of *GSTA1*B* reduced BU CL by 30%	Johnson et al. [27]

AUC area under the curve, *BU* busulfan, *CY* cyclophosphamide, *CI* confidence interval, *CL* Clearance, C_{max} the maximal concentration, C_{ss} the steady state concentration, *FLU* fludarabine, *OR* odds ratio

variability of busulfan CL between Chinese adult patients. Additionally, that also might attribute to different GSTA1 enzymatic activities in patients at different age. Recent studies [6, 25, 27] reported that *GSTA1* genotype played a pivotal role in prediction of initial busulfan doses in pediatric patients. Meanwhile, Abbasi et al. [28] showed that *GSTA1* did not influence busulfan CL obviously in both oral and intravenous administration in adult patients. A higher impact of *GSTA1* genotype on busulfan CL in pediatric patients could be explained by age-specific GSTA1 enzymatic activity [29, 30]. For *GSTA1*, one of drug-processing genes in liver, the highest fold increase in the mRNA expression was induced by the prototypical ligands of xenobiotic-sensing transcription factors during adolescent age. Li et al. [29] highlighted that the drug-processing genes regulation was critical to predict drug PK and to decrease drug toxicity in pediatric patients. This in vitro study demonstrated the importance of *GSTA1* genotype to recommend the initial busulfan dose and to avoid toxicity in children.

We did not find that the other factors, such as *GSTP1*, *GSTM1*, conditioning regimen, body surface area (BSA), and weight, showed a significant impact on busulfan PK. Pharmacogenomics data about busulfan PK in different populations are summarized in Table 4 [6–8, 19, 20, 25–28, 31–45]. Of all, *GSTM1* null genotype and *GSTP1*G* diplotype were commonly reported to have a significant association with busulfan CL [20, 34]. However, Ten Brink et al. [39] did not find an association between the two *GST* genotypes and busulfan CL. This may be related to their minor contribution to busulfan metabolism. For conditioning regimen, Yeh et al. [46] reported a greater interdose variability of busulfan CL in the targeted busulfan–FLU regimen compared to the targeted busulfan–CY regimen ($P=0.0016$). The impact of FLU on busulfan CL was not found in the study of Perkins et al. [47]. PPK analysis of Wu et al. [48] found that BSA significantly influenced the CL and Vd of busulfan in Chinese patients ($P<0.001$, $n=53$). The PPK or PK studies of busulfan in Asian patients were scanty and limited by small sample size and single center. A large-scale and multicenter clinical trial was needed to develop the busulfan PPK model to validate the influencing factors on busulfan PK and to be applicable for more Asian patients.

The *GSTA1* genotype-based PPK model of intravenous busulfan was successfully developed and externally validated in Chinese adult patients. However, the influence of *GSTA1* genotype on busulfan CL is tiny and unlikely to be clinically relevant. We did not suggest the guidance of *GSTA1* genotype on initial busulfan dose in Chinese adult patients undergoing HSCT.

Acknowledgments The authors thank the staff of the Department of Bone Marrow Transplantation, Ruijin Hospital, Shanghai Jiaotong

University School of Medicine, for their collaboration and the use of their facilities.

Author contributions Jiong Hu and Wanhua Yang were in charge of the entire project and reviewed the manuscript. Yidan Sun designed the study and wrote the manuscript. Jingjing Huang performed the study and wrote the manuscript. Chenxia Hao, Ziwei Li, and Wu Liang analyzed the data and interpreted the results. Weixia Zhang and Bing Chen provided the reagents and materials.

Funding This work was funded by the National Natural Science Foundation in China (Grant No. 81503137).

Compliance with ethical standards

Conflict of interest The authors declared no potential conflicts of interest with respect to the research, authorship, and/or publication of this article.

Ethical approval The study protocol was approved by the Ruijin Hospital Research Ethics Committee.

References

1. Ciurea SO, Andersson BS (2009) Busulfan in hematopoietic stem cell transplantation. Biol Blood Marrow Transplant 15(5):523–536
2. Copelan EA, Bechtel TP, Avalos BR et al (2001) Busulfan levels are influenced by prior treatment and are associated with hepatic veno-occlusive disease and early mortality but not with delayed complications following marrow transplantation. Bone Marrow Transplant 27:1121–1124
3. Bolinger AM, Zangwill AB, Slattery JT et al (2000) An evaluation of engraftment, toxicity and busulfan concentration in children receiving bone marrow transplantation for leukemia or genetic disease. Bone Marrow Transplant 25:925–930
4. Lee JW, Kang HJ, Lee SH et al (2012) Highly variable pharmacokinetics of once-daily intravenous busulfan when combined with fludarabine in pediatric patients: phase I clinical study for determination of optimal once-daily busulfan dose using pharmacokinetic modeling. Biol Blood Marrow Transplant. 18(6):944–950
5. Paci A, Vassal G, Moshous D et al (2012) Pharmacokinetic behavior and appraisal of intravenous busulfan dosing in infants and older children. Ther Drug Monit 34(2):198–208
6. Nava T, Rezgui MA, Uppugunduri CRS et al (2017) GSTA1 genetic variants and conditioning regimen: missing key factors in dosing guidelines of busulfan in pediatric hematopoietic stem cell transplantation. Biol Blood Marrow Transplant 23(11):1918–1924
7. Nava T, Kassir N, Rezgui MA et al (2018) Incorporation of GSTA1 genetic variations into a population pharmacokinetic model for IV busulfan in paediatric hematopoietic stem cell transplantation. Br J Clin Pharmacol 84(7):1494–1504
8. Yin J, Xiao Y, Zheng H, Zhang YC (2015) Once-daily i.v. BU-based conditioning regimen before allogeneic hematopoietic SCT: a study of influence of GST gene polymorphisms on BU pharmacokinetics and clinical outcomes in Chinese patients. Bone Marrow Transplant. 50(5):696–705
9. Gibbs JP, Czerwinski M, Slattery JT (1996) Busulfan-glutathione conjugation catalyzed by human liver cytosolic glutathione S-transferases. Cancer Res 56(16):3678–3681
10. Czerwinski M, Gibbs JP, Slattery JT (1996) Busulfan conjugation by glutathione S-transferases alpha, mu, and pi. Drug Metab Dispos 24:1015–1019
11. Hayes JD, Strange RC (2000) Glutathione S-transferase polymorphisms and their biological consequences. Pharmacology 61(3):154–166
12. Palmer J, Mccune JS, Perales MA et al (2016) Personalizing busulfan-based conditioning: considerations from the American Society for Blood and Marrow Transplantation Practice Guidelines Committee. Biol Blood Marrow Transplant 22(11):1915–1925
13. Huang J, Li Z, Liang W et al (2019) Accurate prediction of initial busulfan exposure using a test dose with 2- and 6-hour blood sampling in adult patients receiving a twice-daily intravenous busulfan-based conditioning Regimen. J Clin Pharmacol 59(5):638–645
14. Matsuno K, Kubota T, Matsukura Y, Ishikawa H, Iga T (2004) Genetic analysis of glutathione S-transferase A1 and T1 polymorphisms in a Japanese population. Clin Chem Lab Med 42:560–562
15. Arand M, Muhlbauer R, Hengstler J et al (1996) A multiplex polymerase chain reaction protocol for the simultaneous analysis of the glutathione S-transferase GSTM1 and GSTT1 polymorphisms. Anal Biochem 236:184–186
16. Byon W, Smith MK, Chan P et al (2013) Establishing best practices and guidance in population modeling: an experience with an internal population pharmacokinetic analysis guidance. CPT Pharmacometr Syst Pharmacol 3(2):e51
17. Fernandez HF, Tran HT, Albrecht F et al (2002) Evaluation of safety and pharmacokinetics of administering intravenous busulfan in a twice-daily or daily schedule to patients with advanced hematologic malignant disease undergoing stem cell transplantation. Biol Blood Marrow Transplant 8(9):486–492
18. Mamlouk K, Saracino G, Berryman RB, Fay JW, Pineiro LA, Vance EA et al (2005) Modification of the Bu/Cy myeloablative regimen using daily parenteral busulfan: reduced toxicity without the need for pharmacokinetic monitoring. Bone Marrow Transplant 35:747–754
19. Kusama M, Kubota T, Matsukura Y et al (2006) Influence of glutathione S-transferase A1 polymorphism on the pharmacokinetics of busulfan. Clin Chim Acta 368(1–2):93–98
20. Kim SD, Lee JH, Hur EH et al (2011) Influence of GST gene polymorphisms on the clearance of intravenous busulfan in adult patients undergoing hematopoietic cell transplantation. Biol Blood Marrow Transplant 17(8):1222–1230
21. http://www.ftp.1000genomes.ebi.ac.uk/vol1/ftp/data_collections/1000_genomes_project/release/20190312_biallelic_SNV_and_INDEL/
22. Coles BF, Morel F, Rauch C et al (2001) Effect of polymorphism in the human glutathione s-Transferase A1 promoter on hepatic GSTA1 and GSTA2 expression. Pharmacogenet Genom. 11(8):663–669
23. Ansari M, Lauzon-Joset JF, Vachon MF et al (2010) Influence of GST gene polymorphisms on busulfan pharmacokinetics in children. Bone Marrow Transplant. 45:261–267
24. Sun H, Fadiran EO, Jones CD et al (1999) Population pharmacokinetics. A regulatory perspective. Clin Pharmacokinet. 37(1):41–58
25. Ansari M, Curtis PH, Uppugunduri CRS et al (2017) GSTA1 diplotypes affect busulfan clearance and toxicity in children undergoing allogeneic hematopoietic stem cell transplantation: a multicenter study. Oncotarget. 8(53):90852–90867
26. Ansari M, Huezo-Diaz P, Rezgui MA et al (2016) Influence of glutathione S-transferase gene polymorphisms on busulfan pharmacokinetics and outcome of hematopoietic stem-cell transplantation in thalassemia pediatric patients. Bone Marrow Transplant 51(3):377–383
27. Johnson L, Orchard PJ, Baker KS et al (2008) Glutathione S-transferase A1 genetic variants reduce busulfan clearance in children

undergoing hematopoietic cell transplantation. J Clin Pharmacol 48(9):1052–1062
28. Abbasi N, Vadnais B, Knutson JA et al (2011) Pharmacogenetics of intravenous and oral busulfan in hematopoietic cell transplant recipients. J Clin Pharmacol 51(10):1429–1438
29. Li CY, Renaud HJ, Klaassen CD et al (2016) Age-specific regulation of drug-processing genes in mouse liver by ligands of xenobiotic-sensing transcription factors. Drug Metab Dispos Biol Fate Chem 44(7):1038–1049
30. Lu H, Gunewardena S, Cui JY, Yoo B, Zhong XB, Klaassen CD (2013) RNA-sequencing quantification of hepatic ontogeny and tissue distribution of mRNAs of phase II enzymes in mice. Drug Metab Dispos 41:844–857
31. Terakura S, Onizuka M, Fukumoto M et al (2019) Analysis of glutathione S-transferase and cytochrome P450 gene polymorphism in recipients of dose-adjusted busulfan-cyclophosphamide conditioning. Int J Hematol. https://doi.org/10.1007/s12185-019-02741-8
32. Michaud V, Tran M, Pronovost B et al (2019) Impact of GSTA1 polymorphisms on busulfan oral clearance in adult patients undergoing hematopoietic stem cell transplantation. Pharmaceutics. https://doi.org/10.3390/pharmaceutics11090440
33. Nishikawa T, Yamaguchi H, Ikawa K et al (2019) Influence of GST polymorphisms on busulfan pharmacokinetics in Japanese children. Pediatr Int 61(6):558–565
34. Choi B, Kim MG, Han N et al (2015) Population pharmacokinetics and pharmacodynamics of busulfan with GSTA1 polymorphisms in patients undergoing allogeneic hematopoietic stem cell transplantation. Pharmacogenomics. 16(14):1585–1594
35. Ten Brink MH, Swen JJ, Böhringer S et al (2013) Exploratory analysis of 1936 SNPs in ADME genes for association with busulfan clearance in adult hematopoietic stem cell recipients. Pharmacogenet Genom 23(12):675–683
36. Ten Brink MH, Van BT, Swen JJ et al (2013) Effect of genetic variants GSTA1 and CYP39A1 and age on busulfan clearance in pediatric patients undergoing hematopoietic stem cell transplantation. Pharmacogenomics. 14(14):1683–1690
37. Uppugunduri CRS, Rezgui MA, Diaz PH et al (2014) The association of cytochrome P450 genetic polymorphisms with sulfolane formation and the efficacy of a busulfan-based conditioning regimen in pediatric patients undergoing hematopoietic stem cell transplantation. Pharmacogenomics J. 14(3):263–271
38. Bonifazi F, Storci G, Bandini G et al (2014) Glutathione transferase-A2 S112T polymorphism predicts survival, transplant-related mortality, busulfan and bilirubin blood levels after allogeneic stem cell transplantation. Haematologica 99(1):172–179
39. Ten Brink MH, Wessels JA, Hartigh JD et al (2012) Effect of genetic polymorphisms in genes encoding GST isoenzymes on BU pharmacokinetics in adult patients undergoing hematopoietic SCT. Bone Marrow Transplant 47(2):190–195
40. Elhasid R, Krivoy N, Rowe JM et al (2010) Influence of glutathione S-transferase A1, P1, M1, T1 polymorphisms on oral busulfan pharmacokinetics in children with congenital hemoglobinopathies undergoing hematopoietic stem cell transplantation. Pediatr Blood Cancer 55(6):1172–1179
41. Kim MG, Kwak A, Choi B et al (2019) Effect of glutathione S-transferase genetic polymorphisms on busulfan pharmacokinetics and veno-occlusive disease in hematopoietic stem cell transplantation: a meta-analysis. Basic Clin Pharmacol Toxicol 124(6):691–703
42. Srivastava A, Poonkuzhali B, Shaji RV et al (2004) Glutathione S-transferase M1 polymorphism: a risk factor for hepatic venoocclusive disease in bone marrow transplantation. Blood 104(5):1574–1577
43. Bremer S, Fløisand Y, Brinch L et al (2015) Glutathione transferase gene variants influence busulfan pharmacokinetics and outcome after myeloablative conditioning. Ther Drug Monit 37(4):493–500
44. Ansari M, Rezgui MA, Théoret Y et al (2013) Glutathione S-transferase gene variations influence BU pharmacokinetics and outcome of hematopoietic SCT in pediatric patients. Bone Marrow Transplant 48(7):939–946
45. Zwaveling J, Press RR, Bredius RG et al (2008) Glutathione S-transferase polymorphisms are not associated with population pharmacokinetic parameters of busulfan in pediatric patients. Ther Drug Monit 30(4):504–510
46. Yeh RF, Pawlikowski MA, Blough DK et al (2012) Accurate targeting of daily intravenous busulfan with 8-hour blood sampling in hospitalized adult hematopoietic cell transplant recipients. Biol Blood Marrow Transplant 18(2):265–272
47. Perkins JB, Kim J, Anasetti C et al (2012) Maximally tolerated busulfan systemic exposure in combination with fludarabine as conditioning before allogeneic hematopoietic cell transplantation. Biol Blood Marrow Transplant 18(7):1099–1107
48. Wu X, Xie H, Lin W et al (2017) Population pharmacokinetics analysis of intravenous busulfan in Chinese patients undergoing hematopoietic stem cell transplantation. Clin Exp Pharmacol Physiol 44(5):529–538